

## FORMATION OF THE MECHANISM OF PHOTO-SENSITIVE STRUCTURES WITH BARRIERS OF METAL SEMICONDUCTOR IN PHOTODIODE AND PHOTOVOLTAIC MODE

**Feruz Giasova\***

Physical-Technical Institute of the Scientific Association "Physics-Sun" of the Academy of Sciences of the Republic of Uzbekistan. 100084 Tashkent, Bodomzor yuli st., 2 b.

Article Received on 25/10/2017

Article Revised on 15/11/2017

Article Accepted on 06/12/2017

### \*Corresponding Author

**Feruz Giasova**

Physical-Technical Institute  
of the Scientific Association  
"Physics-Sun" of the  
Academy of Sciences of the  
Republic of Uzbekistan.  
100084 Tashkent,  
Bodomzor yuli st., 2 b.

### ABSTRACT

In this paper, the results of a study of the photosensitivity mechanisms of two-barrier one and two basic structures based on gallium arsenide and silicon with a metal-semiconductor transition with different thicknesses of the base area is considered. The results of the analysis of the photodiode and photovoltaic mode of structures with metal-semiconductor barriers are presented on the basis of the obtained electrophysical characteristics.

**KEY WORDS:** silicon, gallium arsenide, doped, thin-base structure, Schottky barrier, Mott barrier, photodiode mode, photovoltaic mode, isotype, heterojunction, thickness, characteristic, current transfer mechanism, photosensitivity.

### INTRODUCTION

Structures with a metal-semiconductor transition are widely used in various industries, electronic circuits of information and telecommunication systems. Due to the creation of various modified structures with a Schottky barrier, Mott and Bardeen,<sup>[1]</sup> new functional properties of structures with a metal-semiconductor transition are realized. At the moment, low-barrier structures are designed to create microwave detectors without bias, and high operating frequencies are achieved on structures with a Mott barrier:

$$C_{\sigma} = S \left( \frac{q \epsilon \epsilon_0 N}{2(U_K \pm U)} \right)^{1/2} = \frac{\epsilon \epsilon_0 S}{d_{\sigma a3a}},$$

Then we have a Mott barrier. In its base area, electrons are absent even with forward bias, and current transfer is determined by the diffusion mechanism:

$$J = J_s [\exp(qU/kT) - 1]$$

Where the saturation current depends little on temperature, but depends more on the voltage. Low values of the barrier capacity allow higher frequencies to be reached than in the Schottky barrier.<sup>[2]</sup> By using the isotypic heterojunctions containing impurity levels as the base area, large photocurrent values are obtained in the long-wavelength area of the spectrum. By creating structures with two potential barriers, two-sided photosensitivity and photocurrent enhancement were obtained, while the realization of structures based on photovoltaic effects began to attract the attention of researchers.

Interest in structures based on photovoltaic effects is due to the absence of dark currents in them, which makes it possible to process optical and other signals without distortion. Photovoltaic optocouplers began to be created, we can say, the formation of a new direction of semiconductor devices on photovoltaic effects began. In fact, it would be more realistic to create a different special purpose structure for photovoltaic effects, since the physical basis of any device has its own specifics.

To date, noiseless structures sensitive in the infrared (IR) spectral area are of interest, intended for use in various information systems. The search for ways to improve the efficiency of IR photodetectors is gaining momentum, much attention has been paid to studies of the photoelectric characteristics of structures with blocked conductivity<sup>[3,4]</sup> and isotype transitions. However, in them the photosensitivity in the long-wavelength area of the spectrum (1-2  $\mu\text{m}$ ) is reached at certain operating voltages, which causes the occurrence of noise currents. Undoubtedly, in this aspect the implementation of photovoltaic receivers, in which the noise current is practically absent, is of interest.

## MATERIALS AND METHODS

The investigated two-base Ag-N<sup>0</sup> AlGaAs-n<sup>+</sup> GaAs-n<sup>0</sup> GaInAs-Au structure with a base thickness of 350  $\mu\text{m}$  was carried out alternately by growing heterolayers in various processes of liquid epitaxy. In one process, an epitaxial AlGaAs heterojayer is grown on one side of a

<sup>+</sup> GaAs substrate (with a carrier density of  $2 \times 10^{18} \text{ cm}^{-3}$ ), and in another process, an epitaxial heterolayer of  $n^0$  GaInAs is grown on the other side of the same substrate. As a result of repeated heat exposure in the hydrogen flow to the heteroepitaxial  $N^0$  AlGaAs layer, the defects are gettered and subsequently the metal-semiconductor junction obtained on its surface acquires the properties of the Mott barrier.

The photodiode Ag- $N^0$ - $n^+$ - $n^0$ -Au structure (Fig. 1) contains a strongly doped substrate  $n^+$  GaAs-1, which creates heterojunctions on the one hand with the  $N^0$  AlGaAs-2 layer with its continuation of the high-resistivity layer 3 with the space-charge layer-4 formed under the semitransparent barrier layer of Ag-5, and on the other hand with a layer of  $n^0$  GaInAs-6 creating in it a layer of space charge-7 under the potential barrier of Au-8. The formation of an i-layer on the surface part of the  $N^0$  AlGaAs heterolayer can be justified with the help of volt-ampere characteristics.

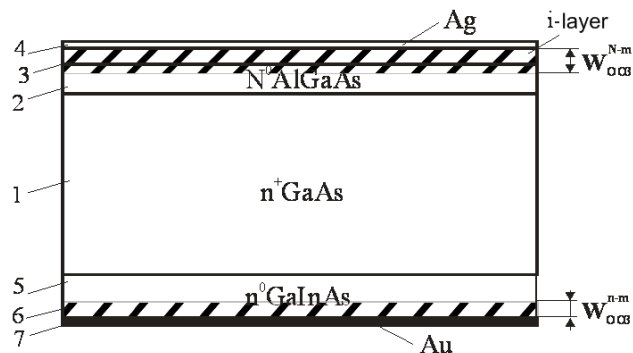


**Fig. 1: Geometry of the heterojunction two-base Ag- $N^0$  AlGaAs- $n^+$  GaAs- $n^0$  GaInAs-Au structure: 1- $n^+$  GaAs, 2.10 cm, 400  $\mu\text{m}$ ; 2- $n^0$  AlGaAs, 4.10 cm, 2  $\mu\text{m}$ ; 3- layer of space charge; Mott's Ag-barrier; 5- $n^0$  GaInAs, 4.10 cm, 1.5  $\mu\text{m}$ ; 6-layer space charge; 7-Au-barrier Schottky.**

The formation of a high-resistance overcompensated i-layer on the surface of  $N^0 \text{ Al}_{0.2} \text{ Ga}_{0.8} \text{ As}$  is associated with its reheating and cooling during the production of the second  $n^0 \text{ Ga}_{0.9} \text{ In}_{0.1} \text{ As}$  heterolayer. In the production of an Ag-metallic contact, an  $m_1$ -i- $N^0$  transition is created on the  $N^0 \text{ Al}_{0.2} \text{ Ga}_{0.8} \text{ As}$  heterolayer surface. As a result, the thickness of the  $N^0 \text{ Al}_{0.2} \text{ Ga}_{0.8} \text{ As}$  heterolayer ( $d_N$ ) consists of the thickness of the space charge layer ( $W_0$ ) created by the barrier ( $m_1$ -i) and the thickness of the quasi-neutral part of the  $N^0 \text{ Al}_{0.2} \text{ Ga}_{0.8} \text{ As}$  hetero-layer ( $d_{\text{quasi}}$ ). The layer of the space charge completely covers the

thickness of the i-layer ( $d_i$ ), which leads to the formation of the Mott barrier ( $W_0 > d_i$ ). The equivalent circuit of the structure under research can be represented as a two-barrier structure with a base area with isotype  $N^0 n^+ n^0$  transitions, that is, it consists of two series isotype transitions, the width of the forbidden band, in which decreases in the direction of the narrow-band part, having 1.67, 1.43, and 1.32 eV. The research of its photoelectric characteristics was carried out by connecting the structure to the power source  $V_1 = U_{num}$  (2) through an ammeter and by measuring the total current and the voltage structure  $V_2 = U_{com}^{m-Nn^+n-m}$  (3) in the dark and when excited by monochromatic radiation.

When illuminated from the wide-band area, photogeneration takes place at the  $Ag-N^0 Al_{0.2} Ga_{0.8} As-n^+ GaAs$  barrier, and the dark  $n^0 Ga_{0.9} In_{0.1} As-Au$  transition becomes a loading resistance, and conversely, when illuminated from the narrow-band side, the dark wide-gap barrier becomes a load. Consequently, the process of the galvanic photocurrent emergence is due to the fact that the dark barriers performs the function as the load resistance, and the illuminated barrier performs the function of the photovoltaic cell. Therefore, when one illuminated surface is replaced by another, we have a photovoltaic current of another transition.

As the wavelength of the exciting optical radiation increases, we first have a photocurrent of one sign generated directly under the barrier and, as the wavelength of the radiation increases, a photocurrent of another sign is created due to the penetration of light radiation into the quasineutral area of the heterolayer of the base. The opposite direction of the generated photocarriers leads to a change in the sign of the photocurrent. Here it should be noted that the photosensitivity of the two-base structure in the photovoltaic mode is governed by a thin-layered heterolayer-heavily doped semiconductor, in addition to settling by the thickness of the base area, also specified by the difference in concentrations on the isotype heterobarrier.

## RESULTS AND DISCUSSION

The photosensitivity mechanism<sup>[6,7]</sup> of the two-base structure can be explained as follows. In the two-base structure, electrons are excited from the side of the illuminated wide-band heterobarrier, which are transferred to the base area, as shown in Fig. 2 position -1, then light from the intrinsic area excites electrons and holes from the depletion layer, which are directed to the base and contact areas (position -2).

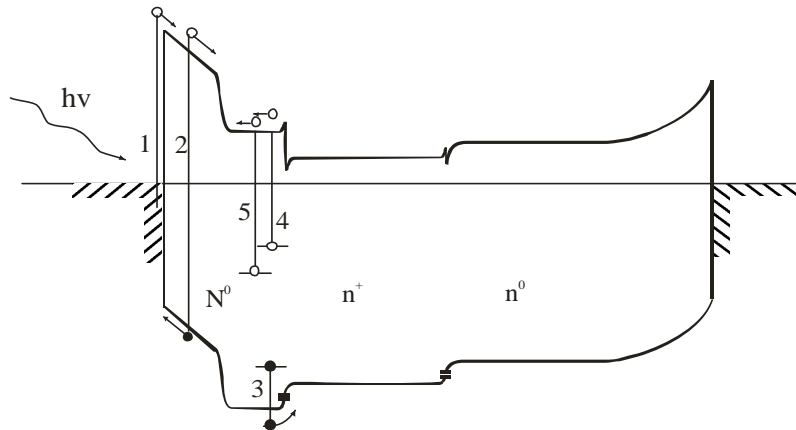


**Fig. 3: Band diagram of the two-base Ag- N<sup>0</sup> Al<sub>0.2</sub> Ga<sub>0.8</sub> As-n<sup>+</sup> GaAs-n<sup>0</sup> Ga<sub>0.9</sub> In<sub>0.1</sub> As-Au structure in the equilibrium state under illumination of the Ag-N<sup>0</sup> Al<sub>0.2</sub> Ga<sub>0.8</sub> As Mott barrier.**

When the wavelength of the radiation is equal with the depth of the impurity level of oxygen, photocarriers from the impurity levels (position-4) begin to be generated. In case of illumination of the Ag-N<sup>0</sup> Al<sub>0.2</sub> Ga<sub>0.8</sub> As-n<sup>+</sup> GaAs-n<sup>0</sup> Ga<sub>0.9</sub> In<sub>0.1</sub> As-Au – structure by the short-wave radiation from the side of the narrow-gap indium-containing heterobarrier the electrons of metal are excited and then with the attainment of the area of intrinsic absorption of photons (Fig. 4, position-1) the electrons and holes are separated (position-2). Subsequently, the carrier is generated from the levels of intrinsic defects (position-3).

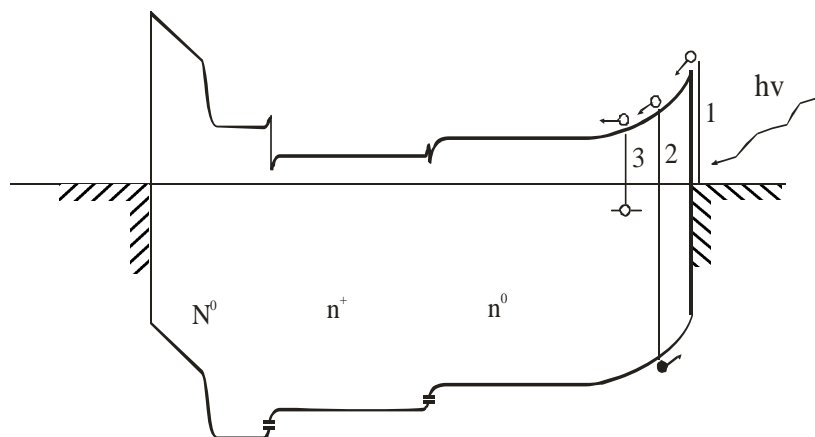


**Fig. 4: Band diagram of the two-base Ag- N<sup>0</sup> Al<sub>0.2</sub> Ga<sub>0.8</sub> As-n<sup>+</sup> GaAs-n<sup>0</sup> Ga<sub>0.9</sub> In<sub>0.1</sub> As-Au structure in the equilibrium state under illumination of a Schottky n<sup>0</sup> Ga<sub>0.9</sub> In<sub>0.1</sub> As-Au barrier.**

A two-barrier photodiode Au-nSi-Al structure based on n-type single-crystal silicon doped with phosphorus with a resistivity of 1 kΩ • cm and a carrier density of  $4.2 \times 10^{14} \text{ cm}^{-3}$  with a

thickness of 570 μm was carried out by vacuum deposition. With the purpose of studying generation-recombination processes in the base area of the structure, we have obtained potential barriers on both surfaces of nSi, since at contacts to nSi the structure turns into a resistor. To obtain rectifying contacts to nSi, Au layers of ~ 100 Å thick were applied to one surface and Al was applied to another surface by evaporation in a vacuum of ~ 10<sup>-7</sup> Torr.

The geometry of the obtained two-barrier Au-nSi-Al structure with collision-crossed transitions is shown in Fig. 4.<sup>[8,9]</sup>

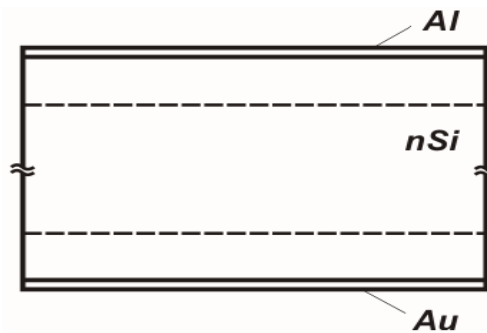


**Fig. 4: Geometric construction Au-nSi-Al-structure.**

From the equivalent circuit from the applied common external voltage to the structure, we will have the total current:

$$I_{COM}^{(+)\text{Au-nSi-Al}(-)} = I_{DIR}^{\text{Au-nSi}} = I_{BACK}^{\text{nSi-Al}}$$

However, the total voltage consists of the sum of the voltages incident at each transition

$$U_{COM}^{(+)\text{Au-nSi-Al}(-)} = U_{DIR}^{\text{Au-nSi}} + U_{BACK}^{\text{nSi-Al}}$$

Volt-ampere characteristics in the mode of direct and reverse bias of the Au-nSi transition at the usual scale are shown in Fig. 5.

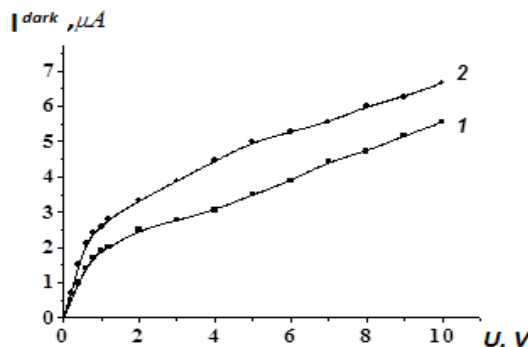


**Fig. 5: Volt-ampere characteristics of the Au-nSi-Al structure on a typical scale with different switching modes: 1 – (-)Au-nSi-Al(+), 2 – (+)Au-nSi-Al(-).**

In accordance with the equivalent circuit (Fig. 4b), when changing the polarity of the operating voltage, the base is alternately locked, then from one side, and from the other, it determines the current flowing through the structure. In this case, the difference in the magnitude of the currents confirms that the metal-semiconductor transitions differ from each other. In our case, due to the use of various metals Au and Al. The dependence of the current on the voltage is described by the power function  $I \sim U$  and is divided into two sections. In the direct shift mode in the first section, the exponent is 0.3, which changes with an exponent of 0.48, and in the locking mode in the first section, the exponent is also 0.3, which is replaced by 0.6. The obtained values of exponents close to 0.5 are inherent in the generation mechanism of current transfer. Using the procedure for determining the incident voltages in each transition,<sup>[9-11]</sup> the values of and are determined in Table 1 based on the experimental data of the current-voltage characteristic.

**Table 1: The calculated data of the voltages incident on the transitions, capacitances and electric field strengths.<sup>[8]</sup>**

<b>(+)Au-nSi-Al(-)</b>						
$U_{COM}^{(+)\text{Au-nSi-Al}(-)}$	$I_{COM}^{\text{Au-nSi-Al}}$	$U_1^{\text{Au-nSi}}$	$U_2^{n\text{Si-Al}}$	$W^{n\text{Si-Al}(-)}$	$E^{n\text{Si-Al}(-)}$	$C^{n\text{Si-Al}(-)}$
V	μA	V	V	cm	V/cm	F
0	0	0	0	0,008583	0	5,19054E-11
0,2	0,7	0,1162	0,0838	0,009596	5,210503	4,64256E-11
0,6	2,1	0,3486	0,2514	0,011831	15,21459	3,76561E-11
1	2,6	0,4316	0,5684	0,015233	28,22785	2,92454E-11
4	4,45	0,7387	3,2613	0,034775	88,66102	1,28109E-11
8	6	0,996	7,004	0,049988	131,7124	8,91219E-12
10	6,667	1,10672	8,89328	0,056059	148,629	7,94698E-12
<b>(-)Au-nSi-Al(+)</b>						
$U_{COM}^{(-)\text{Au-nSi-Al}(+)}$	$I_{COM}^{\text{Au-nSi-Al}}$	$U_1^{\text{Au-nSi}}$	$U_2^{n\text{Si-Al}}$	$W^{(-)\text{Au-nSi}}$	$E^{(-)\text{Au-nSi}}$	$C^{(-)\text{Au-nSi}}$
V	μA	V	V	cm	V/cm	F
0	0	0	0	0,012138	0	3,67026E-11
0,2	0,5	0,15	0,05	0,013349	6,277559	3,33729E-11
0,6	1,4	0,42	0,18	0,01549	16,2301	2,8761E-11
1	1,9	0,57	0,43	0,018886	30,09583	2,35885E-11
4	3,056	0,9168	3,0832	0,036723	88,80814	1,21314E-11
8	4,72	1,416	6,584	0,052222	134,1197	8,53089E-12
10	5,56	1,668	8,332	0,058507	152,0047	7,61453E-12

Table 1 also gives the values of the maximum electric field strength in the locked transitions and the capacitance values, which are calculated from the formula, where cm<sup>2</sup> is the transition area. Here it should be noted that the course of the dependence of the currents in recalculation from the incident voltage exactly repeats the course of the curve from the total

locked voltage (Figure 6), that is, the mechanisms of current transfer<sup>[7,10]</sup> are identical. As can be seen from Fig. 6, curves 1,2,3 in direct-switched transitions the current increases linearly with respect to incident voltages, where the exponents are equal to 1 and characterize the mechanism of current transfer caused by thermionic emission, and in reverse bias the current increases with respect to falling voltages, the exponents are 0, 7 characterize the generation mechanism of current transfer.<sup>[9]</sup>

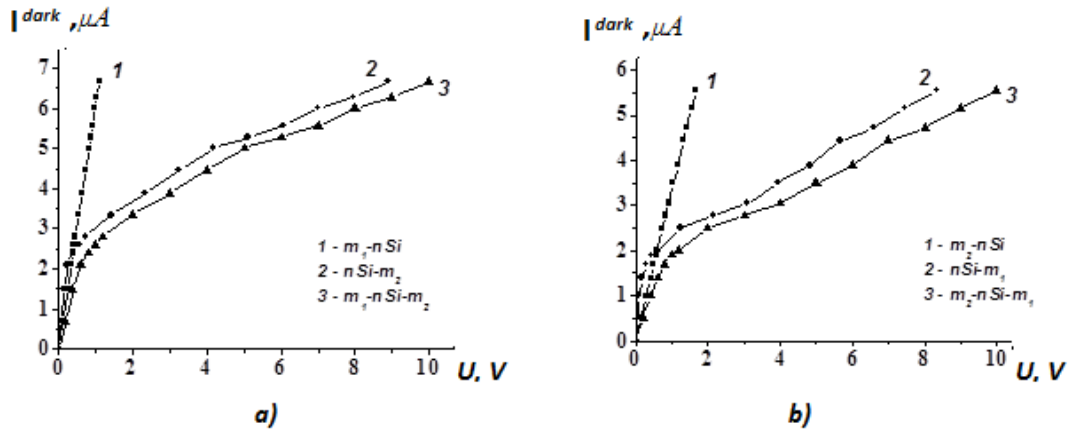


**Fig. 6: Volt-ampere characteristics of the Au-nSi-Al structure at different modes of inclusion from the total voltage and in terms of the voltage of the incident at each transition: a) -(+)Au-nSi-Al(-), b) - (-)Au-nSi-Al(+).**

Since in a direct shift the maximum voltage can not be greater than the value of the contact potential difference, the greater part of the voltage drops in a quasi-neutral part of the base, connected in series with the direct shifting transition, ie. For a given voltage, the thickness of the layers of the space charge is larger on the side of the Au-nSi junction or the set current, also above the electric field strength, Table 1.

Regarding the dependence of capacitance on voltage, it should be noted that the initial capacitance of the Au-nSi junction is less important due to the larger value of the contact potential difference, but as the operating voltage increases, the capacitance values approach.<sup>[9]</sup> The dependence of the spectral sensitivity on the wavelength of monochromatic radiation has a maximum at 1.1 μm, which corresponds to the intrinsic absorption area, Fig. 7.

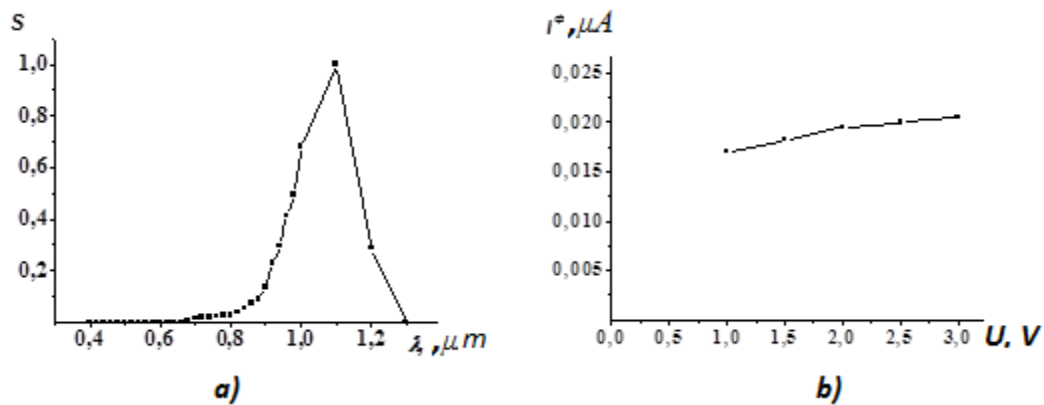


**Fig. 7: Spectral characteristics of the Au-nSi-Al structure (a) and the dependence of the photocurrent on the operating voltage in the intrinsic absorption area (b).**

The magnitude of the spectral photocurrent from the voltage has an increasing character, which is due to the increase in the photo generated carriers in the space-charge area of the locked Au-nSi junction, Fig. 7b. In photodiode mode, the generation of photo carriers is carried out in the Au-nSi-Al structure from the locked metal-semiconductor junction, which is associated with the generation mechanism of current transfer.

## CONCLUSION

Thus, in the investigated two-base Ag-N AlGaAs-n GaAs-n GaInAs-Au structure, the generated photo carriers are directed towards each other at the metal-semiconductor junction and the heterojunction weakly doped-heavily doped semiconductor. In it, the physical processes occurring in one barrier are related to processes taking place in another barrier. In the photodiode Au-nSi-Al structure, the current-voltage characteristics are symmetric, and the mechanisms of current transfer are determined by the generation processes in the space-charge area of the metal-semiconductor barrier. The dependence of the light current on the intensity of illumination is linear. Such structures can be used as photo detectors of large optical signals. Selecting the parameters of the base area (thickness, carrier concentration), contact material, it is possible to obtain multifunctional photo electro conversion structures that are promising for optical communication systems and various optoelectronic devices.<sup>[13,14]</sup>

**REFERENCES**

1. Karimov A.V. Photoelectric amplification in a three-barrier structure. - Laser technology optoelectronics, 1993; 3: 83-85.
2. Averin SV, Stein von Kamensky E., Roskos HG, Kersting R., Pletner D., Gilen H., Kohl A., Spangenberg B., Leo K., Kurz H., Hallricher About Heterobarrier photodiode MPS structures with subpicosecond time resolution // Quantum Electronics. - Moscow, 1994; 21(10): 873-878.
3. Filachev A.M. Taubkin I.I., Trishenkov M.A. Photodetectors in optoelectronic devices and systems. -M.: Fizmatkniga, 2016; 104.
4. Ponomarenko VP, Filachev AM Photodetectors and photodetector modules of a new generation//Applied Physics, 2001; 6: 20-38.
5. Karimov A.V., Yodgorova D.M. Features of Growth Epitaxial Layers of Firm Solutions on a Basis of Indium's and Aluminum's arsenide. Semiconductor Physics Quantum Electronics Optoelectronics. - Kyiv, 2004; 7(4): 383-385.
6. Karimov AV, Yedgorova DM, Giyasova FA, Zoirova L.Kh. Investigation of physical processes occurring in a long base of multi-barrier arsenide-gallium structures. // International Conference: Modern Information and Electronic Technologies (SIET), May 19-23, 2008; Odessa, 2008; 2: 129.
7. Blank TV, Goldberg Yu. A. Mechanisms of current flow in ohmic contacts of metal-semiconductor // FTI., 2007; 41(11): 1281-1308.
8. Abdul Khaev OA, Asanova GO, Yedgorova DM, Yakubov EN, Karimov AV Investigation of the influence of potential barriers on the mechanisms of current transfer in meetings of two-barrier silicon structures, // Physical engineering of a surface, 2011; 9(3): 262-268.
9. Karimov AV, Yedgorova DM, Giyasova FA, Mirdzhalova M., Asanova GO, Abdul Khaev OA, Mukhutdinov Zh. Study of the process of formation of current characteristics of a silicon photodiode with rectifying barriers // Technology and design in electronic equipment, Odessa, 2013; 1: 9-12.
10. Karimov A.V., Yedgorova D.M. Determination of characteristics of two-barrier photodiode structures with metal-semiconductor junctions // Technology and design in electronic equipment, 2005; 5: 27-30.
11. Giyasova F.A. Some features of photoelectric characteristics of silicon photodiode structure. International Journal of Advanced Research in Science, Engineering and Technology, October 2017; 4(10): 4655-4660, Copyright to IJARSET www.ijarset.com

12. S.M. Sze, K.Ng. Kwok. Physics of Semiconductor Devices (Hoboken-New Jersey, Wiley-Interscience, 2007) 3rd ed., 477.
13. Fiber-optical technology: Current state and prospects. 2 nd ed. Pererab. And add. / Sat. articles ed. Dmitreva S.A. and the blind N.N. - Moscow: LLC "Fiber-Optic Technology", 2005; 576.
14. Filachev AM, Ponomarenko VP, Taubkin II, Burlakov ID, Bulgar KO, Gorelik LI, Kravchenko NV, Kulymanov AV, Kulikov KM, Lozhnikov VE, Sharonov Yu.P. Photodetectors and photodetectors for reception of pulsed radiation in the spectral range 0.3 - 11  $\mu\text{m}$  / Applied physics, 2002; 6: 52-61.